Korean J. Chem. Eng., **24**(6), 1106-1112 (2007)

Effect of interaction of operation parameters on elutriation behavior in a vortexing fluidized bed

Chien-Song Chyang, Hou-Peng Wan*,† and Li-Chi Su

Department of Chemical Engineering, Chung Yuan Christian University, Chung-Li, 320, Taiwan, R.O.C.
*Energy & Environment Research Laboratories, Industrial Technology Research Institute (ITRI), Hsinchu, 310, Taiwan R.O.C
(*Received 16 March 2007 • accepted 27 March 2007*)

Abstract−A systematic investigation on elutriation behavior conducted in a vortexing fluidized bed (VFB) cold model is studied. The effects of various parameters on the elutriation are investigated from the data obtained by using 'response surface methodology' (RSM) to determine the relationship between elutriation rate and operating conditions. The results show that all the interactions among primary air flow rate, secondary air flow rate, fine particle size, secondary air inlet diameter, and imaginary circle diameter had significant influences on elutriation behavior in the VFB. The modified regression models of the 'specific elutriation rate constant' (K*) were also submitted in this study.

Key words: Vortexing Fluidized Bed, Elutriation, Response Surface Methodology, Specific Elutriation Rate Constant

INTRODUCTION

The elutriation of fine particles from a fluidized bed is a very important topic in the application of fluidized bed technology. For fluidized bed combustion, the excessive amounts of fly ash and unburned carbon elutriated from the combustor cause poor combustion efficiency and air pollution. Usually, the elutriation rate of fines increases sharply with superficial gas velocity, decreases with the increasing of diameter of the fines, and decreases with the increasing of freeboard height up to a limiting value (TDH; Transport Disengaging Height) [1]. Therefore, how to minimize the elutriation rate from the fluidized bed has become an important issue. The cyclone, recycle system, baffle and other techniques have been used to reduce particles loss, and reported in the literature.

An improved fluidized bed combustion technique, known as the vortexing fluidized bed combustor (VFBC), has been developed for use as a small- or medium-scale boiler or incinerator. The concept of VFBC was originally presented by Sowards [2]. The characteristics of the VFBC can be represented by the swirl flow within the freeboard. To increase the residence time of unburned carbon in the freeboard and prevent the elutriation of fine particles from the fluidized bed, an integration of combustor and cyclone was developed by Korenberg [3]. Based on Korenberg's concept, the vortexing fluidized bed combustor was developed and named by Nieh and Yang [4].

In a pioneer paper, Leva described the elutriation rate of fine particles from a fluidized bed using a first-order rate equation [5]. A 'specific elutriation rate constant', which is independent of bed weight, was presented by Wen and Hashinger to modify Leva's equation. [6] The specific elutriation rate constant is a function of both the operation conditions and geometric structure; therefore, such as the superficial velocity, the secondary air flow, the fine particle size, and the properties of gas and solid are chosen as the operating parameters. According to the published literature, the dominant factors for elutriation are known as the superficial gas velocity, particle size and fluid dynamics within the fluidized bed [7]. Although the elutriation phenomena within a vortexing fluidized bed has been investigated for years, a further, more elaborate study remains needed.

It should be noted that the dependency of the objective function on a certain operating parameter could be various under different conditions. But a full factorial experiment would be nonviable from the viewpoint of time and resources. In this study, the elutriation phenomena will be investigated by using the response surface methodology (RSM), which provides a systematic and efficient experimental strategy. RSM, a fractional factorial experimental design, provides a systematic and efficient experimental strategy for studying the parameter using statistical methods. It has been extensively applied in industrial fields in recent years, such as plasma research [8,9], silica gel manufacturing [10], super conducting generator studies [11], enzyme production [12]; however, the application to the fluidized-bed research field is minimal.

In this study, an attempt was made to investigate the elutriation phenomena in a vortexing fluidized bed cold model using RSM to determine the relationship between elutriation rate and operating conditions. It is known that the specific elutriation rate constant is a function of both the flow situation and geometric structure. Therefore, the primary-air velocity, secondary-air inlet diameter, secondary-air flow rate, the imaginary circle diameter of secondary-air and fine particles diameter are chosen as the operating parameters and processed in terms of two experimental design tables. The specific elutriation rate constant (K*) was assigned as the objective function.

EXPERIMENTAL AND APPARATUS

1. Response Surface Methodology (RSM)

A quadratic polynomial model was used to describe the relationship between the objective function and the operating parameters in the response surface methodology. The general form of a

†To whom correspondence should be addressed.
E-mail: hpwan@itri.org.tw

quadratic model can be represented as:

$$Y = \sum_{i=1}^{n} \beta_{ii} X_i^2 + \sum_{i=1}^{n-1} \sum_{j=i+1}^{n} \beta_{ij} X_i X_j + \sum_{i=1}^{n} \beta_i X_i + \beta_0 \quad (1)$$

where Y is the objective function or response; X_i is the coded operating parameters or factors; n is the factor number. The coefficient values, β_0, β_i, β_{ii}, β_{ij}, were chosen to fit the experimental data well using the least squares method.

In this study, the Box-Behnken design, which is a common experimental design for RSM, was used. A three-factor Box-Behnken design is illustrated in Fig. 1. It is a rotatable spherical design that contains no points at the vertices of the cubic region created by the upper and lower limits for each variable. This could be a great advantage when the points on the corners represent factor-level combinations that are cost-consuming or impossible to execute due to the physical process constraints [13].

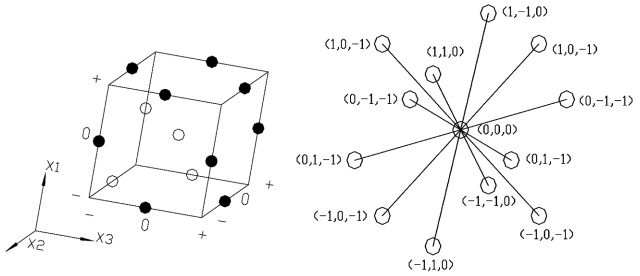

Fig. 1. A three-factor-and-three-level Box-Behnken design.

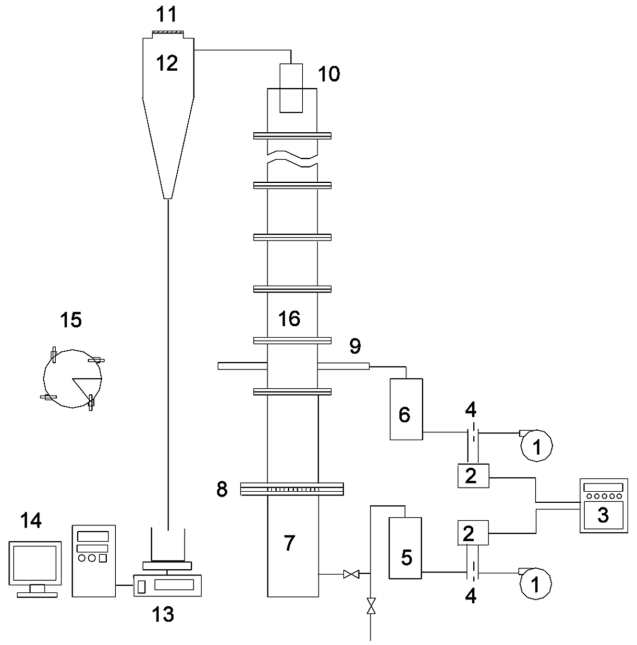

Fig. 2. Schematic diagram of the experimental apparatus.

1. 15 HP Roots blower
2. Pressure transmitter
3. Recorder
4. Orifice plate
5. Humidifier
6. Distributor tank
7. Windbox
8. Gas distributor
9. Secondary air nozzle
10. Gas exhaust tube
11. 300 mesh wire screen
12. Cyclone
13. Electric balance
14. Personal computer
15. Arrangement of secondary air nozzles (top view)
16. Vortexing fluidized bed cold model (0.19 m I.D., 4.0 m Hight)

2. Apparatus

All the experiments were conducted in a vortexing fluidized bed cold model, 0.19 m in diameter, 4.0 m in height and fabricated of a transparent acrylic column. The previous study showed that TDH had been reached at the gas exhaust tube [1]. Two 15 hp roots blowers supplied the flow rate of primary air and secondary air. A schematic diagram of the apparatus is shown in Fig. 2. All experiments were carried out at room temperature (i.e., cold model). In this study, the 'imaginary circle' is defined as an internal tangent circle enclosed by the secondary air nozzles, also as shown in Fig. 3.

3. Powder

Glass beads with density 2,520 kg/m^3 and particle size 545 μm were used as the bed material (coarse particle). According to the experimental design for RSM, glass beads with three sizes of 81, 97, and 113 μm were chosen as elutriated fine particles, which were carried over from the column and captured by a cyclone and weighed continuously. Physical properties of particles used in this study are summarized in Table 1.

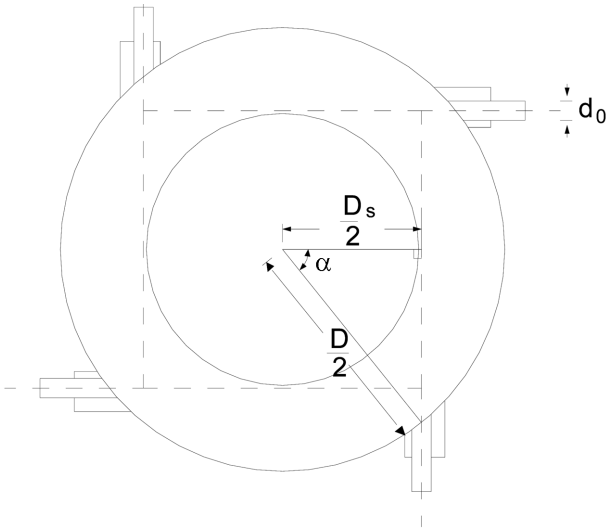

Fig. 3. Schematic diagram of the arrangement of the secondary air nozzles (imaginary circle).

Table 1. Relevant properties of glass beads used in the experiments

Particle size (μm)	ρ (kg/m^3)	U_{mf}[a] (m/s)	U_t[b] (m/s)	Geldart group[c]
Coarse particle (bed material)				
545	2,520	0.220	4.001	B
Fine particles (elutriated particles)				
113	2,520	0.010	0.660	B
97	2,520	0.0078	0.555	B
81	2,520	0.0054	0.452	A

[a]U_{mf} estimated by correlation of Wen and Yu (1966);
[b]U_t calculated by correlation Wen and Hashinger [6];
[c]Drawn largely from Geldart (1972).

Table 2. The experimental factors, and the coded values used in this experiment

Coded levels			Corresponding operating value					
	Symbol	Normalized value	category I			category II		
			U_1 (m/s)	U_2 (m/s)	d_p (μm)	Q_2 (Nm^3/min)	d_o (m)	D_s (m)
low	X_1	−1	1.18	10.2	81	0.7	0.014	0.05
center	X_2	0	1.47	17.6	97	1.2	0.019	0.12
high	X_3	+1	1.76	25.0	113	1.7	0.024	0.19

4. Operation Parameter Design

According to Box-Behnken design, we made two categories for experimental design, which include factors about the particle property and hydrodynamic characteristics within the freeboard. The K* was assigned as the objective function. In Table 2 (category I), three independent parameters, U_1, U_2, d_p, were symbolized as coded factors, X_1, X_2, X_3. In Table 2 (category II), three independent parameters about the secondary air, Q_2, d_o, D_s, were also symbolized as coded factors, respectively.

Three levels were chosen for each factor. In order to make the associated parameter estimates at the same scale for comparison, parameter values were coded as the normalized values −1, 0, and +1. The factors, coded levels and their corresponding operating parameters and values are also shown in Table 2.

Analysis of variance (ANOVA) was carried out by using the commercial package JMP and Minitab. The Student's t-test was used to examine the main effects, quadratic effects and interaction effects of parameters.

5. Calculation of Specific Elutriation Rate Constant

In this study, the elutriation rate equation proposed by Wen and Hashinger was used to describe the elutriation rate.

$$\frac{dC}{dt} = -K^* \frac{A}{W} C \tag{2}$$

where: $K^* = \frac{KW}{A}$

C=fine particle's concentration in the column

$$\text{Since } C = \frac{W_0 - W}{W_T - W} \tag{3}$$

Substituting for C from Eq. (3), Eq. (2) can be integrated as:

$$\ln\left(\frac{W_0 - W}{W_0}\right) = \left(\frac{A}{W_0 - W_T}\right) K^* t \tag{4}$$

Eq. (4) can be used to estimate the specific elutriation rate constant (K*).

An electronic balance was used to weight the fine particles which were elutriated from the column and captured by the cyclone. The elutriated fine particles fell into the breaker that was placed on the electric balance. The accumulated weight of the elutriated fine particles in the beaker was continuously measured by the electronic balance, and the data measured were transferred to a personal computer by using an RS232 interface card. The time interval of data transferred to the personal computer was two seconds. Typical elutriation rate experiment result was illustrated in Fig. 4. The specific elutriation rate constant was the slope of the graph in Fig. 4.

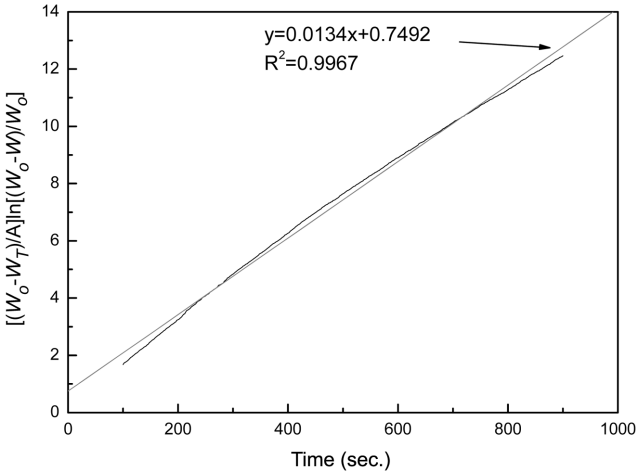

Fig. 4. Typical elutriation rate experiment results (Q_1=2.5 Nm^3/min; Q_2=1.7 Nm^3/min).

Table 3. A three-factor-three-level experimental design

No.	Pattern			Block	X_1		X_2		X_3	
					U_1	Q_2	U_2	d_o	d_p	D_s
1	−	−	0	1	−1		−1		0	
2	−	+	0	1	−1		+1		0	
3	+	−	0	1	+1		−1		0	
4	+	+	0	1	+1		+1		0	
5	0	−	−	1	0		−1		−1	
6	0	−	+	1	0		−1		+1	
7	0	+	−	1	0		+1		−1	
8	0	+	+	1	0		+1		+1	
9	−	0	−	1	−1		0		−1	
10	+	0	−	1	+1		0		−1	
11	−	0	+	1	−1		0		+1	
12	+	0	+	1	+1		0		+1	
13	0	0	0	1	0		0		0	
14	0	0	0	1	0		0		0	
15	0	0	0	1	0		0		0	

RESULTS AND DISCUSSION

1. Analysis of Variance

Based on the Box-Behnken design, fifteen experimental sets were constructed into a fractional factorial experiment. The center point in the experimental design, i.e., a combination of all factors at the center-level, was replicated three times to experimental accuracy.

The three-factor-and-three-level Box-Behnken experimental design is shown in Table 3.

Based on the experimental data, via the multiple variable regression, a polynomial quadratic model or called a second-order response surface model was obtained as follows:

$$\ln(K^*) = -4.27 + 2.36U_{1,c} + 0.24U_{2,c} - 0.36d_{p,c} - 0.31(U_{1,c})^2 - 0.49U_{2,c}U_{1,c} + 0.48(U_{2,c})^2 - 0.63d_{p,c}U_{1,c} + 0.43d_{p,c}U_{2,c} - 0.34(d_{p,c})^2 \quad (5)$$

Where: 1.18 m/s<$U_{1,c}$<1.76 m/s
10.2 m/s<$U_{2,c}$<25.0 m/s
81 μm<$d_{p,c}$<113 μm

$$K^* = 10^{-3} \times [4.47 + 12.4 \times Q_{2,c} + 0.59 \times d_{o,c} - 0.81 \times D_{s,c} + 1.44 \times (Q_{2,c})^2 - 4.51 \times d_{o,c} \times Q_{2,c} + 0.39 \times (d_{o,c})^2 - 5.95 \times D_{s,c} \times Q_{2,c} + 1.35 \times D_{s,c} \times d_{o,c} - 2.01 \times (D_{s,c})^2] \quad (6)$$

Where: 0.7 Nm^3/min<$Q_{2,c}$<1.7 Nm^3/min
0.014 m<$d_{o,c}$<0.024 m
0.05 m<$D_{s,c}$<0.19 m

Table 4. The analysis of variance for the regression models (ANOVA) of category I

Source	DF	Sum of squares	Mean square	F Ratio	Prob.>F
Model	9	51.102821	5.67809	26.5805	0.0011
Error	5	1.068094	0.21362	-	-
Total	14	52.170915	-	-	-

Where: R^2=0.979527, R^2_{adj}=0.942676, Mean Square Error=0.21362

Table 5. The analysis of variance for the regression models (ANOVA) of category II

Source	DF	Sum of squares	Mean square	F Ratio	Prob.>F
Model	9	0.00225763	0.000251	121.2841	<0.0001
Error	5	0.00001034	0.000002		
Total	14	0.00226797			

Where: R^2=0.99544, R^2_{adj}=0.987233, Mean Square Error=0.000002

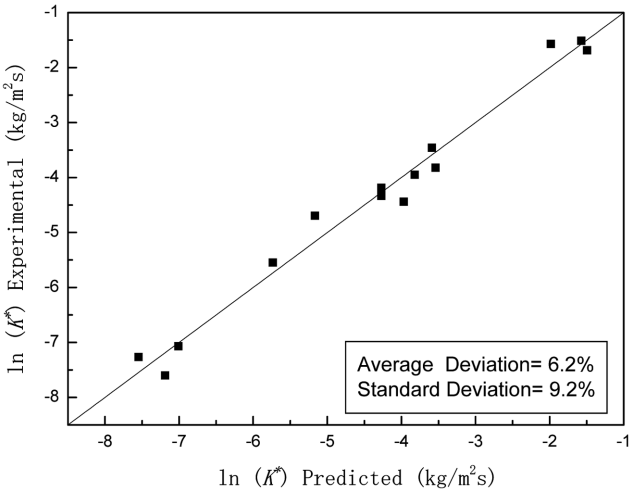

Fig. 5. A comparison of K* experimentally observed with K* predicted by Eq. (5).

The corresponding analysis of variance is tabulated in Tables 4 and 5. The small probability value (P-value) indicates that the experimental data were fitted well by the quadratic model. The determination coefficients, R^2, of 0.98 for Eq. (5) and 0.995 for and Eq. (6) suggest a good fit. A high determination coefficient means the regression model had a good correlation between the model and experimental data.

Comparison of the K* obtained from experimental data with predicted value of K* using Eqs. (5) and (6) is shown in Figs. 5 and 6. From Figs. 5 and 6, a pretty good agreement between them is observed.

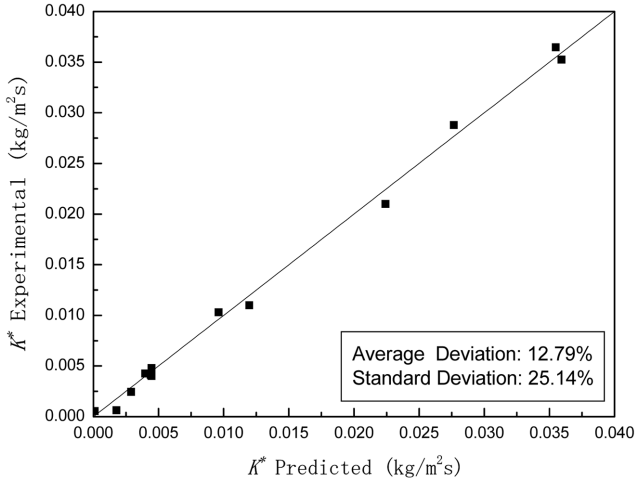

Fig. 6. A comparison of K* experimentally observed with K* predicted by Eq. (6).

Table 6. The effect examinations of the coded factors

Factor	Coefficient	Standard error	*t* Ratio	Prob.>*t*
category I		Confidence interval: 95% (α=0.05)		
Intercept	−4.27	0.27	−16.00	<0.0001
$U_{1,c}$	2.36	0.16	14.45	<0.0001
$U_{2,c}$	0.24	0.16	1.48	0.2001
$d_{p,c}$	−0.36	0.16	−2.19	0.0801
$U^2_{1,c}$	−0.31	0.24	−1.27	0.2596
$U_{2,c} \times U_{1,c}$	−0.49	0.23	−2.10	0.0898
$U^2_{2,c}$	0.48	0.24	1.98	0.1049
$d_{p,c} \times U_{1,c}$	−0.63	0.23	−2.71	0.0423
$d_{p,c} \times U_{2,c}$	0.43	0.23	1.87	0.1209
$d^2_{p,c}$	−0.34	0.24	−1.42	0.2161
category II		Confidence interval: 95% (α=0.05)		
Intercept	0.0045	0.00083	5.38	0.0030
$Q_{2,c}$	0.0124	0.00051	24.29	<0.001
$d_{o,c}$	0.0006	0.00051	1.17	0.2956
$D_{s,c}$	−0.0008	0.00051	−1.59	0.1726
$Q^2_{2,c}$	0.0144	0.00075	19.19	<0.0001
$d_{o,c} \times Q_{2,c}$	−0.0045	0.00072	−6.27	0.0015
$d^2_{o,c}$	0.0004	0.00075	0.52	0.6264
$D_{s,c} \times Q_{2,c}$	−0.0060	0.00072	−8.27	0.0004
$D_{s,c} \times d_{o,c}$	0.0013	0.00072	1.87	0.1198
$D^2_{s,c}$	−0.0020	0.00075	−2.68	0.0437

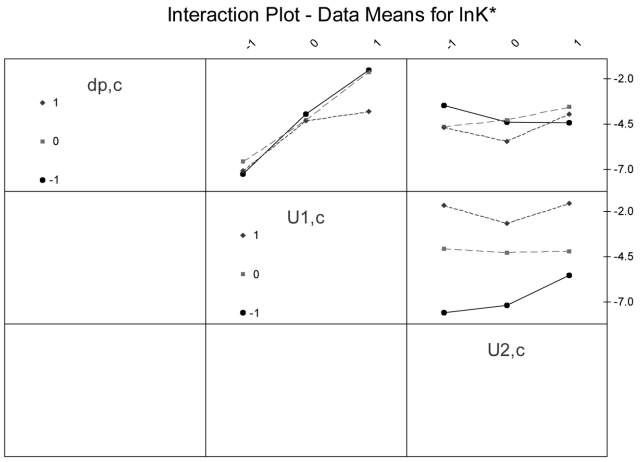

Fig. 7. Interaction plots of Category I ($d_{p,c}$, $U_{1,c}$, $U_{2,c}$).

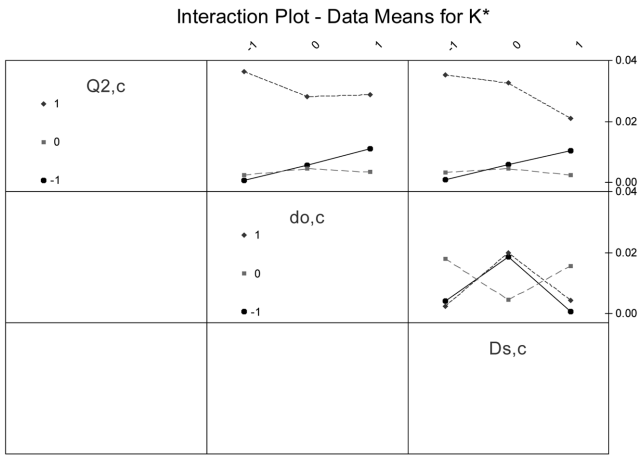

Fig. 8. Interaction plots of Category II ($Q_{2,c}$, $d_{o,c}$, $D_{s,c}$).

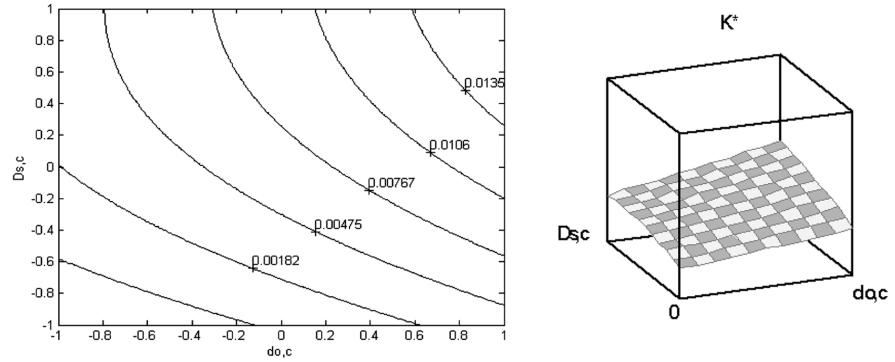

(a) The lower secondary air flow rate; Q_2= 0.7Nm^3/min

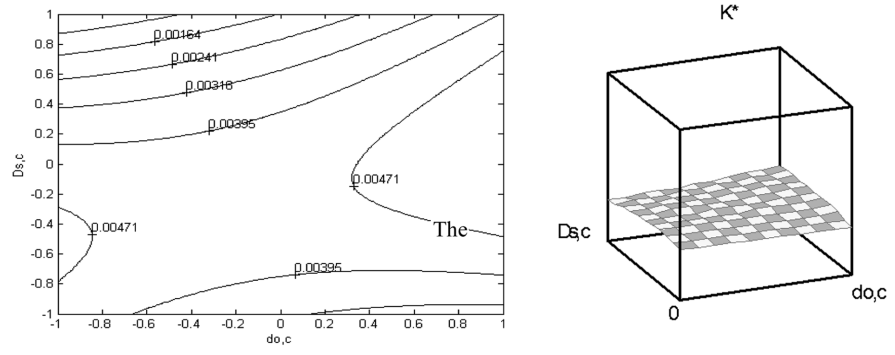

(b) The moderate secondary air flow rate; Q_2= 1.2Nm^3/min

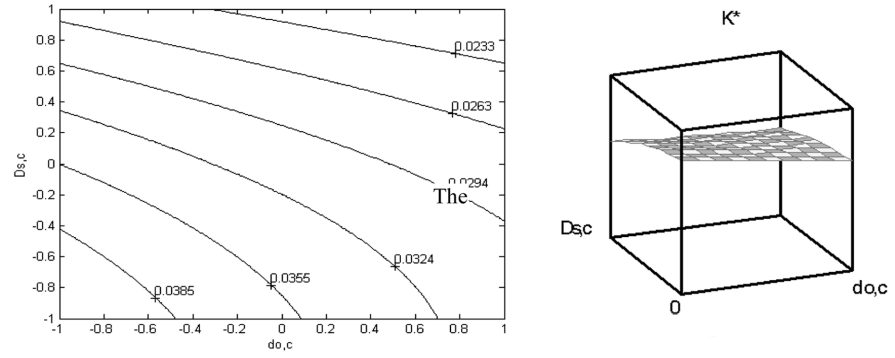

(c) The high secondary air flow rate; Q_2= 1.7Nm^3/min

Fig. 9. The $D_{s,c}$ vs. $d_{o,c}$ contour plot and the corresponding mesh plot with the various secondary air flow rate (Q_2=0.7, 1.2, 1.7 Nm^3/min).

2. Effect Examinations of the Operating Parameters

The effect examinations of the coded factors are tabulated in Table 6. The probability value (P-value) decreases with an increasing absolute t-ratio, or the coefficient to standard-error ratio. A small probability value suggests that the influence of the factor was significant. When the probability value for a factor is greater than 0.05, it means that the influential degree of the factor is lower than the 95% confidence interval.

The probability values of those terms such as the U_1, and $d_{p,c}\times U_{1,c}$ in the category I are lower than 0.05 as shown in Table 6 . It is suggested that these factors have a significant influence on objective function (K^*). Furthermore, the $Q_{2,c}$, $Q^2_{2,c}$, $d_{o,c}\times Q_{2,c}$, $D_{s,c}\times Q_{2,c}$, $D^2_{s,c}$ are confirmed to have significant influence in the category II. Consequently, we can infer that all the interactions between 'primary air and fine particle size', 'secondary-air flow rate and the imaginary circle diameter', and 'secondary-air flow rate and secondary-air inlet diameter' exert great influence on elutriation behavior. The significance of interaction of parameters on the objective function is shown in Figs. 7 and 8.

It is anticipated that the interaction effect between D_s and d_o on K* is significantly strong, as demonstrated in Fig. 9. From Fig. 9, a small secondary-air inlet diameter and small imaginary circle diameter are suggested for decreasing elutriation rate when operating at a lower secondary air flow rate (Q_2=0.7 Nm^3/min). When operating at moderate secondary air flow rate (Q_2=1.2 Nm^3/min), all the experimental data still show an acceptable elutriation rate. It means that when the experiment was operated at a secondary-air inlet diameter around 14-24 mm and imaginary circle diameter around 5-19 cm, a low elutriation rate was obtained while the secondary air flow rate was lower than 1.2 Nm^3/min.

However, if the secondary air flow rate is higher (e.g. Q_2=1.7 Nm^3/min), the elutriation rate increases with the secondary air flow rate. It will need a larger diameter of secondary air nozzle and larger imaginary circle diameter. In this condition, it will get a good performance on lower elutriation quantity. From this point of view, we get a quantitative result from the MATLA program in all experimental operating ranges.

The result shows that when the fluidized bed cold model apparatus is operated at primary airflow rate fixed at 2.5 Nm^3/min and secondary airflow rate is equal to 0.985 Nm^3/min, a secondary air nozzle diameter of 19.19 mm and an imaginary circle diameter of 7.73 cm, a minimum elutriation rate can be obtained.

The general dependency of K^* on each factor is shown in Fig. 10, with the other three factors fixed at the center level. The short vertical bar on the curve represents the 95% confidence interval for the K* value. In Fig. 10, we also can found the relationship between the specific elutriation rate and the coded level of various factors.

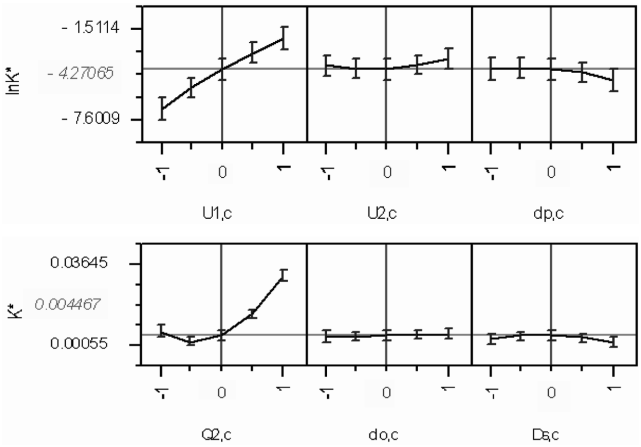

Fig. 10. The general dependency of the elutriation rate on each factor.

3. Evolution of the Response Surface Model

From Table 6, some operation terms in the model may turn out to be less significant in the elutriation behavior; it is adequate to dismiss those terms. A small probability value suggests that the influence of the factors was significant. When the probability value for a factor is greater than 0.05, it means that the influential degree of the factor is lower than the 95% confidence interval. Taking Eq. (5) for instance, three terms out of the fifteen model terms are regarded as significant. Therefore, only these three terms are kept to construct a new model as Eq. (7) for category I.

$$\ln K^* = (-35.57) + 21.23U_1 - 0.13U_1 d_p + 0.20 d_p \quad (7)$$

Where: 1.18 m/s<U_1<1.76 m/s
81 μm<d_p<113 μm

Six terms are regarded significant for category II in the same method. We get a new model after regression once again with the JMP program. It can be expressed as Eq. (8).

$$K^* = (-0.0139) - 0.058\times Q_2 + 0.002\times d_o + 0.003\times D_s + 0.057\times Q_2^2 - 0.0018\times d_o\times Q_2 - 0.0017\times D_s\times Q_2 - 0.00004\times (D_s)^2 \quad (8)$$

Where: 0.7 Nm^3/min<Q_2<1.7 Nm^3/min
0.014 m<d_o<0.024 m

Table 7. The analysis of variance for the modified regression models

Source	D.F.	Sum of squares	Mean square	F Ratio	Prob.>F
Category I		R^2=0.885401, R^2_{adj}=0.866301, Mean Square Error=0.4982			
Model	2	46.19	23.10	46.36	<0.0001
Error	12	5.98	0.50	-	-
Total	14	52.17	-	-	-
Category II		R^2=0.988442, R^2_{adj}=0.982021, Mean Square Error=0.000003			
Model	5	0.00224	0.000448	153.94	<0.0001
Error	9	0.00003	0.000003	-	-
Total	14	0.00227	-	-	-

$0.05\ m<D_s<0.19\ m$

Table 7 shows the result of analysis of variance for the modified regression model. An extremely small probability value (p-value) was obtained, which suggests a good one-order equation relationship. And both determination coefficients (R^2) are higher than 0.9, which means that the equations also have a good resolving ability to experiment data.

CONCLUSIONS

A systematic investigation of particle elutriation conducted in a vortexing fluidized bed cold model is reported. The experimental results show that the significant order of dominant factors is: primary air flow rate, fine particle diameter, secondary air flow rate, the imaginary circle diameter, and secondary air inlet diameter.

All the interactions between primary air flow rate and fine particle size, secondary air flow rate and imaginary circle diameter, and secondary air flow rate and secondary air inlet diameter exert great influences on elutriation quantity.

The modified regression models for category I and category II were submitted in this study. The best operating point is secondary airflow rate (Q_2) equal to 0.985 Nm^3/min, diameter of secondary air nozzle (d_o) equal to 19.19 mm, and diameter of imaginary circle (D_s) equal to 7.73 cm.

NOMENCLATURE

A : cross sectional area of the bed [m^2]
C : fine particle concentration in the bed [m^2]
D : diameter of column [m^2] [-]
D_s : diameter of imaginary circle of the air injection [m]
d_o : diameter of the secondary air nozzles [m]
d_p : mean diameter of particles [m]
K^* : the specific elutriation rate constant [kg/m^2s]
Q_2 : the secondary air flow rate [Nm^3/min]
U_1 : superficial gas velocity [m/s]
U_2 : the secondary air velocity in the VFB [m/s]
U_{mf} : minimum fluidized velocity of particles [m/s]
U_t : terminal velocity of particles [m/s]
W : weight of elutriation particles [kg]
X_i : the coded factors in the Box-Behnken experimental design, i=1, 2, 3 [-]
Y : the objective function or response

Greek Letters

α : subtended angle of imaginary circle with the column in Fig. 3 [rad]
b_o, b_i, b_{ii}, b_{ij} : coefficient values in Eq.(1) [-]
ρ : particle density [kg/m^3]

Under Marks

c : the coded variable [-]
o : initial [-]

REFERENCES

1. H.-P. Wan and C.-S. Chyang, *J. Chem. Eng. Japan*, **31**(6), 977 (1998).
2. Sowards, N. K., *Pollution incineration of solid waste*, US Patent No. 4,060,041 (1977).
3. J. Korenberg, *Proc. 4th. Int. Conf. on Fluidization*, D. Kunii and R. Tori, Eds., Japan, 491-498 (1983).
4. S. Nieh and G. Yang, *Powder Technol*., **50**, 121 (1987).
5. M. Leva, *Chem. Eng. Progr.*, **47**(1), 39 (1951).
6. C. Y. Wen and R. F. Hasinger, *AIChE J.*, **6**, 220 (1960).
7. H.-P. Wan and C.-S. Chyang, *Korean J. Chem. Eng.*, **16**, 654 (1999).
8. S. Agarwala, O. King, S. Horst, R. Wilson and D. Stone, *J. Vac. Sci. Technol*., **A17**(1), 52 (1999).
9. R. Wächter and A. Cordery, *Carbon*, **37**, 1529 (1999).
10. T. W. Chung, T. S. Yeh and T. C. K. Yang, *J. Non-Crystal. Solids*, **279**(1-3), 145 (2001).
11. Y. K. Kim, Y. S. Jo, J. P. Hong and J. Lee, *Cryogenics*, **41**, 39 (2001).
12. W. C. Chen and C. H. Liu, *Enzyme and Microbial Technol.*, **18**, 153 (1996).
13. D. C. Montgomery, *Design and analysis of experiments*, 4th Ed., John Wiley & Sons, New York (1997).